Calculus of the Elastic Properties of a Beam Cross-Section

Alessandra Genoese [1], Andrea Genoese[*,2], Giovanni Garcea[3]
Dipartimento di Modellistica per l'Ingegneria, Universitá della Calabria
Universitá della Calabria, Via P. Bucci - Cubo 39C, 87036 Arcavacata di Rende (CS), *AndreaGenoese_83@hotmail.it

Abstract: Saint-Venánt general rod theory is used to calculate the elastic factors of a section through the numerical solution of a system of partial differential equations. The elastic properties so evaluated are used in a geometric nonlinear analysis of 3D beam structures with general cross-section to calculate some important quantities such as the stiffness matrix. Linear solutions, such as the Saint-Venánt one, can be exploited in this context too due to corotational strategies that allow the generation of objective nonlinear structural models reusing the information gained from the linear ones by applying a corotational reference frame that follows the rigid body motion of the element or, as in a new approach called implicit corotational [5], of the continuum point or of the beam section. A series of tests regarding 3D beam analysis are presented and comparisons with the results obtained using commercial codes such as ABAQUS show the simplicity and accuracy achieved with the proposed formulation.

Keywords: Saint-Venánt rod theory, Elastic factors of a beam cross-section.

1 Introduction

Saint-Venánt (SV) rod theory represents a powerful theoretical basis for the study of slender bodies subjected to general loading conditions. This classical elastic problem still attracts numerous researchers, principally because all kinds of rod analyses, when described as one-dimensional bodies, require the preliminary evaluation of the elastic properties of the cross-section. While the axial and bending factors can be easily obtained, the description of the torsional and shear behavior require the solution of a set of 2D Laplace differential equations on the section domain with Neumann boundary conditions.

The aim of this work is the calculus of the elastic properties of beams with general cross-sections extending the approach proposed by Petrolo and Casciaro in [3] to the evaluation of all the coefficients required by the geometric nonlinear analysis of 3D beam structures.

The reuse of classical linear elastic solutions, such as the SV one, in the nonlinear context is possible due to the well known corotational strategy (CR) or to the more recent proposal of the implicit corotational method (ICR) [5]. The latter, in particular, appears to be very attractive due to the possibility of completely reusing the available linear models, as a basis for generating appropriate nonlinear ones. Today the great majority of nonlinear beam models are based on the so called *geometric exact theories* such as those developed by Reissner [7], Antmann [1] and Simo [8]. These models use direct assumptions of constitutive laws in terms of stress/strain resultants and simplified kinematics and static hypothesis. Models so generated are geometrically exact, that is exactly frame–invariant, but often lack the richness of the 3D solution by omitting important details covered by the linear 3D solution of the same model. This is evident, for example, in the classical Antman–Simo nonlinear beam model where the simplified elastic constitutive law assumed misses the correct shear/torsional coupling present in the 3D Saint Venánt linear solution [6] or more subtle nonlinear couplings such as the axial-torsional 2nd–order coupling identified by Wagner [9]. On the contrary, corotational strategies recover all the effort spent in developing linear theories such as for example the SV one in the nonlinear context and then overcome the inconvenience deriving from separate ad hoc derivations of their nonlinear version. This possibility could be exploited at the finite element level (CR) or, as recently proposed in [4, 5], at the continuum description level (ICR). In the first case, each element is referred to a local frame that moves with the element to filter a great amount of its rigid motion, while ICR applies the corotational description to the neighbor of each continuum point (or to the cross-section in the case of

beam structures): in a suitable corotational reference frame, linear stress and strain measures can be assumed as the Biot nonlinear ones. In this way, a standard methodology to obtain a frame–invariant nonlinear modeling able to maintain all the richness of the embedded linear theory could be derived.

The paper is organized as follows:

section 2 contains an essential overview of the axial and shear stress distribution on the cross-section domain derived from Saint-Venánt assumptions. The latter are defined through three functions ψ_j that solve the Laplace differential equation for different Neumann boundary conditions;

section 3 shows how the elastic factors can be derived once these functions are known by defining the complementary strain unitary energy;

section 4 discusses the procedure followed to calculate the torsional and shear factors. The modulus COMSOL Multiphysics - PDE was used;

section 5 presents the results of some numerical tests performed to show both the reliability and the accuracy achieved with the proposed formulation. Two groups of tests are proposed: in the first one the cases of a rectangular section, a trapezoidal compact section and a bridge section are considered to compare the elastic factors calculated with the available reference values, while in the second one the compliance operators obtained through COMSOL are used in the nonlinear analysis of 3D beam structures. The equilibrium-paths are compared with those obtained using the commercial code ABAQUS.

Final comments and remarks are given in section 6, while appendix A deals with the principal shear system.

2 The stress distribution

Let's consider a cylindrical Cauchy isotropic body subjected to surface loading on its end sections, as shown in figure 1. The cylinder is referred to a local barycentric Cartesian system $\{x, y, z\}$ oriented according to the principal directions of the cross-section and we denote with A the cross-section domain in the $\{x, y\}$ plane, Γ its contour and n_x, n_y the components of the external normal $\boldsymbol{n}$. Saint-Venánt assumptions imply

$$\sigma_{xx} = \sigma_{yy} = \tau_{xy} = 0$$

.

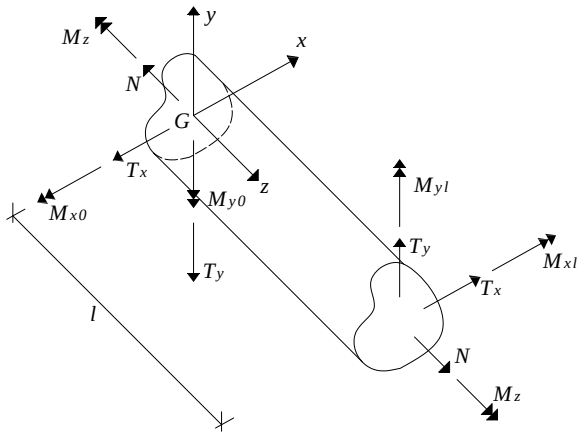

Figure 1: Saint-Venánt cylinder.

The stress field can be expressed in the form

$$\sigma_{zz} = \boldsymbol{D}_\sigma \boldsymbol{t}_\sigma \,, \quad \boldsymbol{\tau} = \left\{ \begin{matrix} \tau_{xz} \\ \tau_{yz} \end{matrix} \right\} = \boldsymbol{D}_\tau \boldsymbol{t}_\tau, \quad (1)$$

where

$$\begin{aligned} &\boldsymbol{t}_\sigma = \left\{ \begin{matrix} N \\ M_x[z] \\ M_y[z] \end{matrix} \right\} \,, \quad \boldsymbol{t}_\tau = \left\{ \begin{matrix} T_x \\ T_y \\ M_z \end{matrix} \right\}, \\ &\boldsymbol{D}_\sigma = \left[1/A, \quad y/J_x, \quad -x/J_y \right], \\ &\boldsymbol{D}_\tau = \left[\boldsymbol{d}_x, \quad \boldsymbol{d}_y, \quad \boldsymbol{d}_z \right]. \end{aligned} \quad (2)$$

N, T_x, T_y are the normal and shear forces, $M_x[z]$, $M_y[z]$, M_z the bending couples and the torque on the cross-section of area A and bending moments of inertia

$$J_x = \int_A y^2 \, dA \,, \quad J_y = \int_A x^2 \, dA \,.$$

Vectors $\boldsymbol{d}_x$, $\boldsymbol{d}_y$, $\boldsymbol{d}_z$ are defined as

$$\left\{ \begin{aligned} \boldsymbol{d}_x &= \nabla \psi_x - \boldsymbol{b}_x - r_x \boldsymbol{d}_z \\ \boldsymbol{d}_y &= \nabla \psi_y - \boldsymbol{b}_y - r_y \boldsymbol{d}_z \\ \boldsymbol{d}_z &= (\nabla \psi_z - \boldsymbol{b}_z)/r_z \end{aligned} \right. \quad (3)$$

∇ is the gradient operator in the $\{x, y\}$ plane, so that

$$\nabla \psi_j = \left\{ \begin{matrix} \dfrac{\partial \psi_j}{\partial x} \\ \dfrac{\partial \psi_j}{\partial y} \end{matrix} \right\} \,, \quad j = x, y, z,$$

while

$$\boldsymbol{b}_x = \frac{1}{2\,J_y}\left\{\begin{array}{c} x^2 - \bar{\nu} y^2 \\ 0 \end{array}\right\},$$
$$\boldsymbol{b}_y = \frac{1}{2\,J_x}\left\{\begin{array}{c} 0 \\ y^2 - \bar{\nu} x^2 \end{array}\right\}, \qquad (4)$$
$$\boldsymbol{b}_z = \frac{1}{2}\left\{\begin{array}{c} y \\ -\,x \end{array}\right\},$$

$$r_j = 2\int_A \{\boldsymbol{b}_j - \nabla\psi_j\}^T \boldsymbol{b}_z dA\,, \quad j = x, y, z. \qquad (5)$$

Finally $\bar{\nu} = \nu/(1+\nu)$ depends on the Poisson coefficient ν of the material.

Functions $\psi_j[x, y]$ have to satisfy the differential problems:

$$\left\{\begin{array}{l} \dfrac{\partial^2\psi_j}{\partial x^2} + \dfrac{\partial^2\psi_j}{\partial y^2} = 0, \;\; \{x, y\} \in A \\ \dfrac{\partial\psi_j}{\partial x}\, n_x + \dfrac{\partial\psi_j}{\partial y}\, n_y = \boldsymbol{b}_j^T \boldsymbol{n}, \;\; \{x, y\} \in \Gamma \end{array}\right. \qquad (6)$$

A detailed discussion of the Saint-Venánt problem with a complete proof of the expressions given is available in [3] or [2].

3 Cross-section flexibility matrixes

In [3] the elastic properties of the cross-section are defined by introducing the unitary energy

$$\frac{\partial\phi}{\partial z} = \frac{1}{2E}\int_A \sigma_{zz}^2\, dA \; + \frac{1}{2G}\int_A \boldsymbol{\tau}^T\boldsymbol{\tau}\, dA \qquad (7)$$

E being the Young modulus and $G = \dfrac{E}{2(1+\nu)}$ the tangential elasticity modulus of the material.

Equations (1) and (2) can be introduced in the energy expression (7) which gives

$$\frac{\partial\phi}{\partial z} = \frac{1}{2E}\boldsymbol{t}_\sigma^T\boldsymbol{H}_\sigma\boldsymbol{t}_\sigma \; + \frac{1}{2G}\boldsymbol{t}_\tau^T\boldsymbol{H}_\tau\boldsymbol{t}_\tau, \qquad (8)$$

being the global strengths acting on the cross-section independent from x and y.

Symmetric matrixes $\boldsymbol{H}_\sigma$ and $\boldsymbol{H}_\tau$ introduced in equation (8) can be calculated as

$$\boldsymbol{H}_\sigma = \int_A \boldsymbol{D}_\sigma^T\boldsymbol{D}_\sigma\, dA\,, \quad \boldsymbol{H}_\tau = \int_A \boldsymbol{D}_\tau^T\boldsymbol{D}_\tau\, dA \qquad (9)$$

and have components

$$\boldsymbol{H}_\sigma = diag\left[\frac{1}{A}\,, \quad \frac{1}{J_x}\,, \quad \frac{1}{J_y}\right]$$
$$H_{\tau ij} = \int_A \boldsymbol{d}_i^T\boldsymbol{d}_j\, dA. \qquad (10)$$

In the case of symmetric cross-sections, $\boldsymbol{H}_\tau$ is a diagonal matrix and its components provide the shear and torsional factors A_x^*, A_y^*, J_t used in technical applications directly:

$$\boldsymbol{H}_\tau = diag\left[\frac{1}{A_x^*}\,, \quad \frac{1}{A_y^*}\,, \quad \frac{1}{J_t}\right], \qquad (11)$$

while in the hypothesis of general cross-section we need to introduce the shear principal system to calculate the shear and torsional factors. This operation is, however, not difficult, once the coefficients $H_{\tau ij}$ are known (more details are available in Appendix A).

4 Use of COMSOL Multiphysics

The modulus COMSOL Multiphysics - PDE was used to solve the problems (6) and calculate the integrals (9) on the cross-section domain. In particular the following quantities are defined:

- A 2D geometry in which x and y are the independent variables;
- Quantities ν and $\bar{\nu}$ as constants;
- The three terms $\boldsymbol{b}_j^T\boldsymbol{n}$ as Boundary Expressions;
- Quantities useful to obtain the area and the bending moments of inertia and the expressions of r_j between the Integration Coupling Variable on the domain;
- The components of vectors $\boldsymbol{d}_j$ and the dot products $\boldsymbol{d}_i^T\boldsymbol{d}_j$ on the domain;
- The three differential Laplace equations for the domain and the Neumann conditions for the contour;
- A mesh for the domain using Lagrange-Quadratic elements.

Having solved the problems (6), the Postprocessing menu is very useful to evaluate the integrals $H_{\tau ij}$.

The elastic compliance matrixes $\boldsymbol{H}_\sigma$ and $\boldsymbol{H}_\tau$ so evaluated are a good approximation of the nonlinear compliance operators (see [4, 5]), used in the analysis of structures undergoing large displacements and rotations but small strains, when a suitable corotational reference system or a suitable stress definition is chosen.

5 Numerical Results

5.1 Validation tests

Three tests are presented relating to the rectangular, the trapezoidal and the composed sections in figures 2, 3 and 4 in order to show the performances of the proposed formulation in the evaluation of the elastic factors.

In the first case the numerical values of $k_x = \frac{A}{A_x^*}$, $k_y = \frac{A}{A_y^*}$, $k_t = \frac{J_p}{J_t}$, J_p being the polar inertia, are in perfect agreement with the available analytical values ($k_x = k_y = 6/5$ for $\nu = 0$ and $k_t = 1.82204$ for any ν).

For the trapezoidal and the bridge sections proposed, the flexural systems indicated in red are defined by $d_1 = 1.8571$, $d_2 = 1.2857$, $\alpha = 1.1695\, rad$ and $d = 2.1552$ respectively. They do not coincide with the shear systems indicated in blue. The numerical results obtained (tables 2 and 3) agree with those proposed in [3] where different discretization strategies have been investigated.

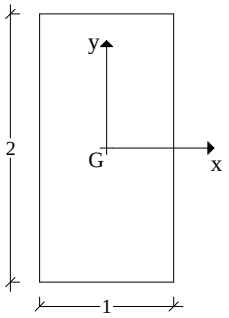

Figure 2: Rectangular cross-section.

	$\nu = 0.0$	$\nu = 0.3$	$\nu = 0.5$
k_x	1.2000	1.2748	1.3561
k_y	1.2000	1.2006	1.2012
k_t		1.8220	

Table 1: Rectangular section.

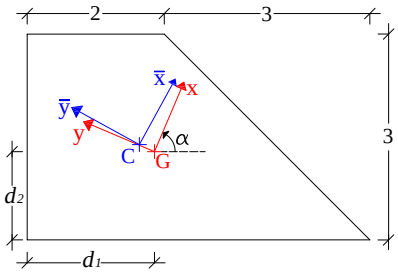

Figure 3: Trapezoidal cross-section.

	$\nu = 0.0$	$\nu = 0.3$	$\nu = 0.5$
k_x	1.3468	1.3771	1.4100
k_y	1.1841	1.1856	1.1871
k_t		1.6481	
x_c		0.0091	
y_c		0.2429	
$\alpha_t(rad)$	-0.0996	-0.0847	-0.0729

Table 2: Trapezoidal compact section.

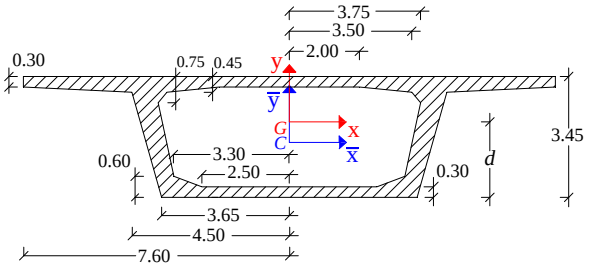

Figure 4: Bridge section.

k_x	k_y	k_t	y_c
1.6686	4.3291	4.4489	-0.5863

Table 3: Bridge section ($\nu = 0.3$).

5.2 Comparison tests

The tests regard the cantilever beams whose geometry and elastic modula are reported in figures 5 - 8. In the first case a lateral force λ is applied at the centroid of the edge of the beam, while the second cantilever is subjected to the axial load λ also applied at the centroid of the edge with a lateral imperfection $\varepsilon\lambda$. ε was assumed to be 0.001. COMSOL was used in performing the calculus of the compliance operators $\boldsymbol{H}_\sigma$ and $\boldsymbol{H}_\tau$ for the C-shaped and the asymmetric cross-sections of the cantilevers required in the analysis of the 3D beam as proposed in [5]. The two tests confirm the accuracy of that beam model in thin walled structure analysis through a comparison with the results furnished by ABAQUS where the cantilevers were modeled as plate-assemblages.

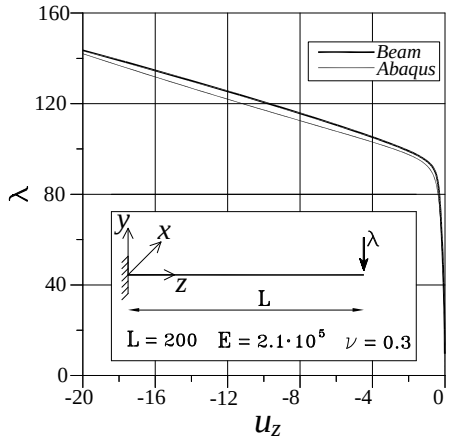

Figure 5: C-shaped beam under shear force: geometry and equilibrium path. Axial displacement u_z at the edge of the beam.

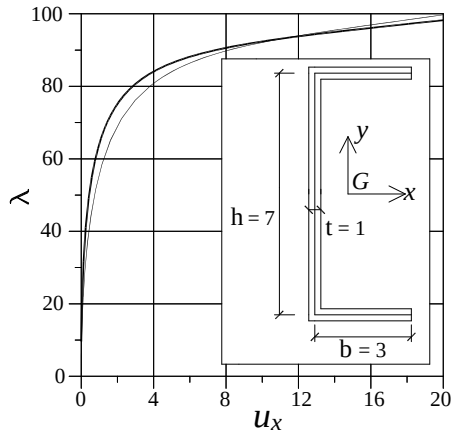

Figure 6: C-shaped beam under shear force: geometry and and equilibrium path. Lateral displacement u_x at the edge of the beam.

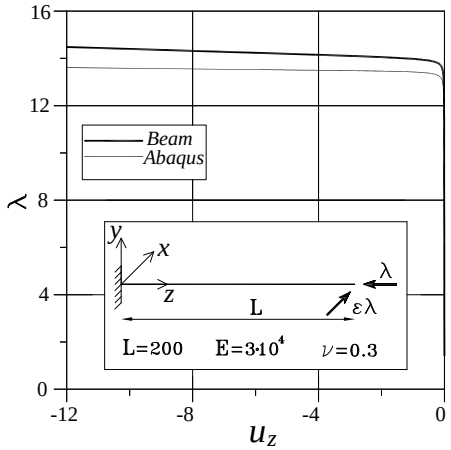

Figure 7: Asymmetric cross-section beam under axial force: geometry and and equilibrium path. Axial displacement u_z at the edge of the beam.

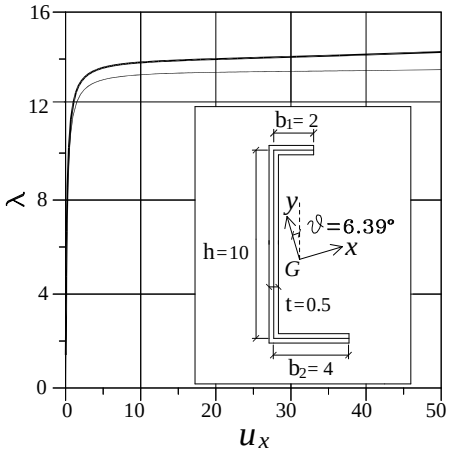

Figure 8: Asymmetric cross-section beam under axial force: geometry and and equilibrium path. Lateral displacement u_x at the edge of the beam.

6 Conclusion

The possibility to evaluate the beam section elastic compliance matrixes in a simple way and reuse these quantities for the nonlinear analysis of 3D beams gives a series of advantages with respect to the classical beam models that use a simplified elastic law on the section and allows a complete and accurate recovery of the rich linear solution in a nonlinear context.

In [5] a 3D nonlinear beam model is derived from Saint-Venánt rod theory and a mixed finite element with a separate interpolation for section strengths and displacements is proposed. The comparisons performed confirm its reliability and accuracy: the numerical results obtained in the analysis of systems constituted by slender beams agree with those furnished by more complex structural modelings such as the shell one. Furthermore, in ABAQUS only a path-following approach is used while the proposed beam element is introduced in an asymptotic background of FEM analysis that offers numerous advantages such as the negligible extra-cost in performing imperfection sensitivity analysis.

Appendix A: The shear system

In the case of general cross-section, the shear stress energy is written in the more usual technical form

$$\frac{\partial \phi_T}{\partial z} = \frac{1}{2G}\left\{\frac{\bar{T}_x^2}{A_x^*} + \frac{\bar{T}_y^2}{A_y^*} + \frac{\bar{M}_z^2}{J_t}\right\}, \qquad (12)$$

where

$$\begin{aligned} \bar{T}_x &= T_x\, c + T_y\, s, \\ \bar{T}_y &= -T_x\, s + T_y\, c, \\ \bar{M}_z &= M_z + T_x\, y_c - T_y\, x_c \end{aligned} \qquad (13)$$

are the principal components of shear strength and the torsional moment referring to the shear center of coordinates

$$x_c = -\frac{H_{\tau 23}}{H_{\tau 33}}\,, \quad y_c = \frac{H_{\tau 13}}{H_{\tau 33}}. \qquad (14)$$

c and s are the cosine and the sine of the deviation angle α_t between shear and flexural systems that can be calculated by using the relation

$$\tan(\alpha_t) = \frac{c_2 - c_1 + \sqrt{c_2^2 - 2c_1c_2 + c_1^2 + 4c_3^2}}{2c_3}, \qquad (15)$$

where

$$\begin{aligned} c_1 &= H_{\tau 11} - 2H_{\tau 13}\, y_c + H_{\tau 33}\, y_c^2, \\ c_2 &= H_{\tau 22} + 2H_{\tau 23}\, x_c + H_{\tau 33}\, x_c^2, \\ c_3 &= H_{\tau 12} + H_{\tau 13}\, x_c - H_{\tau 23}\, y_c - H_{\tau 33}\, x_c y_c. \end{aligned} \qquad (16)$$

The expressions furnished can be obtained by writing the shear forces and the torque referring to the principal system of the cross-section as a function of $\bar{T}_x$, $\bar{T}_y$, $\bar{M}_z$ as follows:

$$\boldsymbol{t}_\tau = \boldsymbol{T}\bar{\boldsymbol{t}}_\tau, \qquad (17)$$

with

$$\begin{aligned} \boldsymbol{T} &= \begin{bmatrix} c & -s & 0 \\ s & c & 0 \\ s\,x_c - c\,y_c & s\,y_c + c\,x_c & 1 \end{bmatrix}, \\ \bar{\boldsymbol{t}}_\tau &= \begin{Bmatrix} \bar{T}_x \\ \bar{T}_y \\ \bar{M}_z \end{Bmatrix}. \end{aligned} \qquad (18)$$

The shear contribution to the unitary energy (8) is then

$$\frac{\partial \phi_T}{\partial z} = \frac{1}{2G}\bar{\boldsymbol{t}}_\tau^T \bar{\boldsymbol{H}}_\tau \bar{\boldsymbol{t}}_\tau, \qquad (19)$$

where

$$\bar{\boldsymbol{H}}_\tau = \boldsymbol{T}^T \boldsymbol{H}_\tau \boldsymbol{T}. \qquad (20)$$

Equation (19) is equal to (12) if $\bar{\boldsymbol{H}}_\tau$ is a diagonal matrix: the conditions of independence of the shear forces and the torque ($\bar{H}_{\tau 13} = \bar{H}_{\tau 23} = 0$) furnish the shear center coordinates, while the angle α_t can be obtained by imposing the independence between $\bar{T}_x$ and $\bar{T}_y$ ($\bar{H}_{\tau 12} = 0$). Finally, the diagonal terms allow the calculation of the necessary shear and torsional factors. They are

$$\begin{aligned} A_x^* &= \frac{1}{c_1\, c^2 + c_2\, s^2 + 2\, c_3\, c\, s} \\ A_y^* &= \frac{1}{c_1\, s^2 + c_2\, c^2 - 2\, c_3\, c\, s} \\ J_t &= \frac{1}{H_{33}}, \end{aligned} \qquad (21)$$

References

[1] S.S. Antman, *Nonlinear problems of elasticity*, Springer-Verlag, New-York, 1995.

[2] R. Baldacci, *Scienza delle costruzioni*, vol. 1, UTET, Torino, 1983.

[3] A. S. Petrolo R. Casciaro, *3d beam element based on saint-venant rod theory*, Computers & Structures **82** (2004), 2471–2481.

[4] G. Garcea A. Madeo G. Zagari R. Casciaro, *Asymtotic postbuckling fem analisys using corotational formulation*, Journal of Solid and Structures **46** (2009), pp. 377–397.

[5] G. Garcea A. Madeo R. Casciaro, *The implicit corotational method, part I/II*, submitted to Computer Methods in Applied Mechanics and Engineering.

[6] Barré de Saint Venánt, *Mémoires sur la torsion des prismes, avec des considérations sur la flexion*, Mémoires des savants étrangers **14** (1955), pp. 233.

[7] E. Reissner, *On one-dimensional finite strain beam theory: the plane problem*, J. Appl. Math. Phys **23** (1972), pp. 795–804.

[8] J.C. Simo, *A three dimensional finite-strain rod model. part ii: Computational aspect*, Computer Methods in Applied Mechanics and Engineering **58** (1986), pp. 79–116.

[9] H. Wagner, *Torsion and buckling of open section*, NACA TM 807, 1936.